

Spin-lattice-electron dynamics simulations of magnetic materials

Pui-Wai Ma* and S. L. Dudarev

EURATOM/CCFE Fusion Association, Culham Science Centre, Abingdon, Oxfordshire OX14 3DB, United Kingdom

C. H. Woo

Department of Electronic and Information Engineering, The Hong Kong Polytechnic University, Hong Kong SAR, China

(Received 16 January 2012; revised manuscript received 5 April 2012; published 1 May 2012)

We develop a dynamic spin-lattice-electron model for simulating the time-dependent evolution of coupled spin, atomic, and electronic degrees of freedom in a magnetic material. Using the model, we relate the dissipative parameters entering the Langevin equations for the lattice and spin degrees of freedom to the heat transfer coefficients of a phenomenological spin-lattice-electron three-temperature model. We apply spin-lattice-electron dynamics simulations to the interpretation of experiments on laser-induced demagnetization of iron thin films, and estimate the rates of heat transfer between the spins and electrons, and between atoms and electrons. To model the dynamics of energy dissipation in a magnetic material undergoing plastic deformation, we develop an algorithm that separates the local collective modes of motion of atoms from their random thermal motion. Using this approach, we simulate the propagation of compressive shock waves through magnetic iron. We also explore the microscopic dynamics of dissipative coupling between the spin and lattice subsystems, and show that the rate of spin-lattice heat transfer is proportional to the integral of the four-spin time-dependent correlation function.

DOI: [10.1103/PhysRevB.85.184301](https://doi.org/10.1103/PhysRevB.85.184301)

PACS number(s): 75.10.Hk, 02.70.Ns, 62.20.-x, 75.50.Bb

I. INTRODUCTION

Magnetic materials have diverse applications ranging from nanoscale magnetic devices to alloys and steels developed for applications in fission and fusion power generation. Various physical properties of these materials depend on the microscopic hierarchical energy relaxation processes involving not only the atomic, but also the magnetic and electronic degrees of freedom. Modeling the dynamics of such relaxation processes poses significant computational challenges since one needs to consider interactions between the thermal excitations of several different microscopic degrees of freedom within a self-consistent simulation framework.

Körmann *et al.*¹⁻³ have highlighted the significance of the magnetic contribution to the free energy of a magnetic material. They evaluated the total free energies and heat capacities of Fe, Co, and Ni using CALPHAD for the electron and lattice subsystems, and quantum Monte Carlo for the spin subsystem. The results agree well with experimental data, confirming the significant part played by spin excitations. At the same time, the method described in Refs. 1-3 is only applicable to the treatment of equilibrium time-independent configurations, and does not consider interaction between various degrees of freedom in the material.

A quantum-mechanical algorithm for treating the dynamics of coupled spin and lattice degrees of freedom was proposed by Antropov *et al.*⁴ The method combines *ab initio* molecular dynamics (MD)⁵ and *ab initio* spin dynamics (SD).⁶⁻⁸ The algorithm has the advantage of being able to follow the evolution of electronic structure, although the system size accessible to a practical simulation is still limited to a few hundred atoms. Also, the algorithm does not treat nonequilibrium electronic excitations. A semiclassical algorithm, combining MD and SD, and capable of simulating the coupled dynamics of atoms and spins on a million-atom scale, was developed in Ref. 9.

Finnis *et al.*¹⁰ and Caro and Victoria¹¹ proposed models for energy losses of fast ions, where either a temperature-

dependent dissipative term¹⁰ or a full stochastic Langevin equation treatment¹¹ were included in a classical MD simulation framework. Duffy and Rutherford¹² extended Caro and Victoria's approach and linked MD to a heat transfer equation, which included a heat diffusion term, in order to model electronic subsystem with spatially varying temperature. Race *et al.*^{13,14} investigated, using a tight-binding approach, the microscopic dynamics of energy transfer from a fast ion to the electrons, and concluded that a classical Langevin equation model provides a suitable mathematical framework for the treatment of interaction between the electrons and the atoms.

Langevin dynamics treats thermal excitations by introducing fluctuation and dissipation terms in the equations of motion for the particles or spins. These terms drive the system to thermal equilibrium. Brownian motion¹⁵⁻¹⁷ is probably the best known example of application of the model. Langevin dynamics for spins was developed in Refs. 18-26, and its application to a large system of interacting spins were considered in Refs. 9, 26 and 27.

Skubic *et al.*²⁸ introduced two Langevin thermostats in the spin equations of motion to model the evolution of spins coupled to electrons, on the one hand, and to the lattice, on the other hand. Radu *et al.*²⁹ investigated the solutions of coupled heat transfer equations for the lattice and electron subsystems, treating spin-electron interactions through a fluctuation term in the spin equations of motion. Both models^{28,29} focused on the treatment of the dynamics of spins. The mechanical response of the lattice to the dynamics of spins, or vice versa, was not included in the simulations.

Phenomenological models, such as the three temperature model (3TM)³⁰ or the recently proposed microscopic 3TM³¹, describe interactions between the lattice, spin, and electronic subsystems within a nonequilibrium thermodynamics-based approach. There is significant experimental effort on laser-induced demagnetization,³⁰⁻³⁷ focused on the analysis of relaxation mechanisms involving spin, lattice, and electronic

subsystems, which aims at clarifying the fundamental nature of microscopic relaxation processes in all the three subsystems.^{31,33–40}

In Refs. 9 and 41 we developed a spin-lattice dynamics (SLD) simulation model for a magnetic material, which integrates coupled equations of motion for the atoms and atomic magnetic moments (spins). In the SLD model, the spin and lattice subsystems are explicitly coupled through a coordinate-dependent exchange function, and the temperatures of atoms and spins are controlled by the corresponding Langevin thermostats. This paper extends the simulation methodology to the treatment of spin, lattice, and electronic degrees of freedom within a unified *atomistic* model. This makes it possible to consider the effects of magnetic and electronic excitations on the atomic-level deformation of the lattice. In addition to simulating the elastic response of the material, the model is capable of addressing problems involving plastic deformation, such as dislocation nucleation, formation of defects, and phase transitions. So far, magnetism has remained an entirely unexplored phenomenon in the simulations of shock waves⁴² or collision cascades^{12,43} in magnetic materials, for example, iron-based alloys and steels, where magnetic excitations are known to influence the relative stability of phases,^{44,45} the structure of defects,^{46,47} and high-temperature mechanical properties.^{48–51}

Using the model described below, we are able to identify and quantify parameters that determine the strength of coupling between the spins and electrons, and between the lattice and electrons. Our simulations are able to match, at the quantitative level of accuracy, the dynamics of laser-induced demagnetization observed in experiments on iron thin films.³² Our results are also in agreement with predictions derived from the 3TM model, where the spin, lattice, and electron temperatures are monitored throughout the entire duration of the relaxation process. We note that developing such a microscopic treatment necessarily requires knowing how the effective instantaneous spin temperature is defined in terms of spin directions.²⁷

We start by revisiting the lattice-electron (LE) model. We derive a relationship between the damping constant entering the Langevin equation for the lattice, and the heat transfer coefficient of the 2TM. We then extend the approach to the treatment of the spin subsystem, and map the microscopic spin-lattice-electron model onto the 3TM. Using the equations of motion for spins and atoms, and combining them with a heat transfer equation describing the electrons, we develop a self-consistent spin-lattice-electron dynamics (SLED) simulation model. Fitting the relaxation curves, predicted by the SLED simulations of laser-induced demagnetization, to experiment, we are able to find the numerical values of parameters characterizing the strength of dissipative spin-electron and lattice-electron coupling. We also develop a new approach to modeling mechanical deformations of magnetic materials, which includes the effect of electronic dissipation, and apply it to the simulation of high-speed deformation of iron under shock wave loading conditions. Finally, we develop a microscopic treatment of heat transfer between the spin and lattice subsystems, mediated by spin fluctuations, and show that the rate of spin-lattice relaxation is a functional of the time-dependent four-spin correlation function.

II. LATTICE-ELECTRON DYNAMICS

A. Spatially homogeneous case

Molecular dynamics (MD) is a powerful simulation tool for investigating the complex dynamics of defects on the atomic scale. Its applications include modeling interstitial atom and vacancy migration, simulation of motion of line dislocations and dislocation loops, and their interactions. In a metal, conduction electrons give the dominant contribution to thermal conductivity. Consequently, the heat dissipation through the electronic subsystem has a significant effect on the dynamics of atoms. For example, the residual population of mobile defects formed in a collision cascade turns out to be lower¹² if dissipation into the electronic subsystem is high. This is due to the lattice-electron coupling leading to faster cascade quenching and more pronounced defect clustering and recombination.⁵²

Nevertheless, coupling between electrons and the lattice is not normally taken into account in MD simulations. A natural way of incorporating thermal coupling between electrons and atomic lattice in MD is via Langevin dynamics,^{11,12} where the electronic subsystem is treated as a heat reservoir for the lattice subsystem. Duffy *et al.*¹² generalized the Langevin model to the case of spatially varying electron temperature, described by a heat transfer equation that includes a heat diffusion term. They also derived a relationship between the damping parameter entering the Langevin equation, and the heat transfer coefficient of the LE model, by equating the energy lost by the atoms and the energy gained by the electrons during a single simulation time step.

We start our analysis by mapping the Langevin equations of motion onto a heat transfer equation, considering a nonmagnetic spatially homogeneous case first. Modeling the metal as interacting atoms immersed in a Fermi liquid of conduction electrons, we may write the full Hamiltonian of atoms and electrons in the form

$$\mathcal{H} = \mathcal{H}_l + \mathcal{H}_e, \quad (1)$$

where

$$\mathcal{H}_l = \sum_i \frac{\mathbf{p}_i^2}{2m} + U(\mathbf{R}) \quad (2)$$

is the Hamiltonian of the collection of interacting atoms, and \mathcal{H}_e is the Hamiltonian of conduction electrons. Here \mathbf{p}_i is the momentum of atom i , $U(\mathbf{R})$ is the interatomic potential, and $\mathbf{R} = \{\mathbf{R}_1, \mathbf{R}_2, \dots, \mathbf{R}_N\}$ are the positions of atoms.

The interatomic potential $U(\mathbf{R})$ in Eq. (2) describes electrostatic interaction between the ions as well as chemical bonding associated with the overlap of electronic orbitals. The representation of the energy of interaction in the form of an ion-coordinate-dependent interatomic potential assumes the validity of the adiabatic approximation, where the electron wave function is fully determined by the positions of atoms. At a finite temperature we also need to include the effects of electronic excitations, which modify the electronic structure in the vicinity of the Fermi level. The second term \mathcal{H}_e in (1) describes such excitations, in the approximation where conduction electrons are treated as gas of quasiparticles, which do not contribute to forces acting on atoms.

Without specifying an explicit form of \mathcal{H}_e , we assume that the dissipation and fluctuation forces in the Langevin equations of motion for the atoms result from interaction between the lattice and conduction electrons:

$$\frac{d\mathbf{R}_i}{dt} = \frac{\mathbf{p}_i}{m}, \quad (3)$$

$$\frac{d\mathbf{p}_i}{dt} = -\frac{\partial U}{\partial \mathbf{R}_i} - \frac{\gamma_{el}}{m} \mathbf{p}_i + \mathbf{f}_i. \quad (4)$$

In the above equations γ_{el} is a damping parameter and \mathbf{f}_i is a δ -correlated fluctuating force, satisfying the conditions $\langle \mathbf{f}_i \rangle = 0$ and $\langle f_{i\alpha}(t) f_{j\beta}(t') \rangle = \mu_{el} \delta_{ij} \delta_{\alpha\beta} \delta(t - t')$. Here angular brackets denote averaging over statistical realizations of random forces, μ_{el} characterizes the amplitude of fluctuations of those forces, and subscripts α and β denote the Cartesian components of a vector.

The rate of change of the energy of the lattice atoms E_l can be evaluated using Eqs. (2), (3), and (4), namely

$$\frac{dE_l}{dt} = \sum_i \left(\frac{\mathbf{p}_i}{m} \cdot \mathbf{f}_i - \gamma_{el} \frac{\mathbf{p}_i^2}{m^2} \right). \quad (5)$$

Consider the ensemble average on Eq. (5). The first term in the right-hand side of (5) explicitly depends on the stochastic forces. We evaluate its ensemble average by using the Furutsu-Novikov theorem,^{53–57} similarly to how it was done in Ref. 27. The ensemble-average value of the second term is evaluated using the equipartition principle. This gives

$$\frac{d\langle E_l \rangle}{dt} = \frac{3N\mu_{el}}{2m} - \frac{3N\gamma_{el}k_B T_l}{m}, \quad (6)$$

where N is the total number of atoms and T_l is the lattice temperature.

According to the fluctuation-dissipation theorem (FDT),^{15–17} if a system is in thermal equilibrium with its reservoir then $\mu_{el} = 2\gamma_{el}k_B T_l$. Since μ_{el} characterizes the magnitude of fluctuating forces acting on the lattice subsystem, we assume that these forces result from the interaction with the electronic subsystem, the temperature of which is T_e . Following Refs. 11 and 12 we write the FDT relation as $\mu_{el} = 2\gamma_{el}k_B T_e$, which remains valid even if $T_e \neq T_l$. Equation (6) now becomes

$$\frac{d\langle E_l \rangle}{dt} = \frac{3Nk_B\gamma_{el}}{m} (T_e - T_l). \quad (7)$$

Comparing (7) with the macroscopic heat transfer equations describing energy exchange between the lattice and electronic subsystems in the spatially homogeneous limit, we write

$$C_l \frac{dT_l}{dt} = G_{el}(T_e - T_l), \quad (8)$$

$$C_e \frac{dT_e}{dt} = G_{el}(T_l - T_e), \quad (9)$$

where $C_l = \partial \langle E_l \rangle / \partial T_l$ and $C_e = \partial \langle E_e \rangle / \partial T_e$ are the lattice and electronic specific heats, respectively. Usually, G_{el} is assumed to be a constant parameter if the value of T_e is close to T_l . Recognizing the fact that the notion of temperature is rigorously defined only if a system is in equilibrium, here we treat temperature as a local variable in the nonequilibrium thermodynamics sense. The validity of the heat transfer equation is justified by the assumption that the system is in quasiequilibrium, where locally its energy

distribution function has the same form as in equilibrium, with hydrodynamic coefficients T_e and T_l being slowly varying functions of the spatial coordinates and time.^{58,59}

Comparing Eqs. (7) and (8) we find that the electron-lattice heat transfer coefficient is

$$G_{el} = \frac{3k_B\gamma_{el}}{m\Omega}, \quad (10)$$

where $\Omega = V/N$ is the volume per atom. This equation relates the damping constant γ_{el} , entering the atomic equations of motion, and the macroscopic heat transfer coefficient G_{el} . Equation (10) shows that G_{el} is directly proportional to γ_{el} , in agreement with the earlier work by Duffy *et al.*¹² At the same time, our derivation is different from, and is more general than, the derivation given in Ref. 12. For example, below we show how the same approach can be applied to the treatment of dynamics of spins exchanging energy with the electronic subsystem of the material.

One should note that although here γ_{el} and μ_{el} are treated as constants, they can in fact be functions of T_e , and this assumption would not affect the derivation given above. Since G_{el} is directly proportional to γ_{el} , it can also be treated as a function of T_e . On the other hand, G_{el} could also be a function of T_l , if higher order or nonlinear dissipation terms were included in Eq. (4).

B. Spatially inhomogeneous case

Relaxation to equilibrium may occur even if the local temperature of the electrons is the same as the local temperature of the lattice. In a nonequilibrium configuration involving, for example, laser heating or a thermal spike associated with a collision cascade, temperatures of both the electron and the lattice subsystems are local quantities and are functions of both the time and spatial coordinates.

To define the local temperatures of atoms and electrons, we separate the entire system into regions. We rewrite the lattice Hamiltonian (2) as follows:

$$\mathcal{H}_l = \sum_{i \in A} \frac{\mathbf{p}_i^2}{2m} + \sum_{i \in A^c} \frac{\mathbf{p}_i^2}{2m} + U_A(\mathbf{R}) + U_{A^c}(\mathbf{R}), \quad (11)$$

where A refers to a certain region of the system and A^c refers to its complement. Using the Langevin equations of motion (3) and (4), we find that the rate of energy change in region A is

$$\frac{dE_{l,A}}{dt} = f_{l,A}(\mathbf{R}, \mathbf{p}) + \sum_{i \in A} \left(\frac{\mathbf{p}_i}{m} \cdot \mathbf{f}_i - \gamma_{el} \frac{\mathbf{p}_i^2}{m^2} \right), \quad (12)$$

where

$$f_{l,A}(\mathbf{R}, \mathbf{p}) = \sum_{i \in A^c} \frac{\mathbf{p}_i}{m} \cdot \frac{\partial U_A}{\partial \mathbf{R}_i} - \sum_{i \in A} \frac{\mathbf{p}_i}{m} \cdot \frac{\partial U_{A^c}}{\partial \mathbf{R}_i}. \quad (13)$$

This function depends on $\mathbf{R} = \{\mathbf{R}_1, \mathbf{R}_2, \dots, \mathbf{R}_N\}$ and $\mathbf{p} = \{\mathbf{p}_1, \mathbf{p}_2, \dots, \mathbf{p}_N\}$, but does not depend on Langevin stochastic forces. It describes the energy exchange between various regions in the lattice subsystem only, through the interactions among atoms. The electronic subsystem does not play any part in this energy exchange.

Taking the ensemble average and comparing the result with the spatially inhomogeneous heat transfer equations

$$C_l \frac{dT_l}{dt} = \nabla(\kappa_l \nabla T_l) + G_{el}(T_e - T_l), \quad (14)$$

$$C_e \frac{dT_e}{dt} = \nabla(\kappa_e \nabla T_e) + G_{el}(T_l - T_e), \quad (15)$$

where κ_l and κ_e are thermal conductivities for the lattice and electronic subsystems, we find the same expression for the heat transfer coefficient G_{el} as in the spatially homogeneous case, taking into account that the term $\langle f_{l,A}(\mathbf{R}, \mathbf{p}) \rangle$ describes energy exchange between region A and the rest of the system, and hence corresponds to the heat diffusion terms $\nabla(\kappa_l \nabla T_l)$.

Here we do not derive a relationship between the terms $\langle f_{l,A}(\mathbf{R}, \mathbf{p}) \rangle$ and $\nabla(\kappa_l \nabla T_l)$, as this is not necessary for the development of our model. In principle, this can be performed by carefully mapping the microscopic model to the phenomenological model for heat transfer. The meaning of the two models and their evolution are very similar. Energy exchange between regions via microscopic forces acting at the atomic level is equivalent to diffusion of energy driven by the temperature gradient at the macroscopic level. Here κ_l is assumed to be a function of T_l only.

Combining Eqs. (3), (4), and (15) we arrive at a lattice-electron (LE) dynamics simulation model. The LE model describes a closed system for which the total energy is conserved. The fluctuating force in Eq. (4) depends on T_e , and the spatially varying lattice temperature in (15) is defined as $T_l = 2/(3k_B N_A) \sum_{i \in A} (\mathbf{p}_i^2/2m)$, where N_A is the number of atoms in region A .

III. SPIN-LATTICE-ELECTRON DYNAMICS

A. Equations of motion for the coupled subsystems

In a magnetic material, in addition to the lattice and electronic degrees of freedom, one needs to consider directional spin excitations. The Hamiltonian now has the form

$$\mathcal{H} = \mathcal{H}_l + \mathcal{H}_s + \mathcal{H}_e, \quad (16)$$

where \mathcal{H}_l and \mathcal{H}_e are defined in the same way as in the LE model above, and \mathcal{H}_s is the Hamiltonian for the spin subsystem. For the spins we use a generic Heisenberg Hamiltonian, which describes a broad variety of magnetic materials

$$\mathcal{H}_s = -\frac{1}{2} \sum_{i,j} J_{ij}(\mathbf{R}) \mathbf{S}_i \cdot \mathbf{S}_j. \quad (17)$$

Here \mathbf{S}_i is a spin vector and $J_{ij}(\mathbf{R})$ is a coordinate-dependent exchange coupling function.^{9,60–62} Values of J_{ij} can be found from *ab initio* calculations.^{60–62}

The corresponding Langevin equations of motion have the form⁹

$$\frac{d\mathbf{R}_k}{dt} = \frac{\mathbf{p}_k}{m}, \quad (18)$$

$$\frac{d\mathbf{p}_k}{dt} = -\frac{\partial U}{\partial \mathbf{R}_k} + \frac{1}{2} \sum_{i,j} \frac{\partial J_{ij}}{\partial \mathbf{R}_k} \mathbf{S}_i \cdot \mathbf{S}_j - \frac{\gamma_{el}}{m} \mathbf{p}_k + \mathbf{f}_k, \quad (19)$$

$$\frac{d\mathbf{S}_k}{dt} = \frac{1}{\hbar} [\mathbf{S}_k \times (\mathbf{H}_k + \mathbf{h}_k) - \gamma_{es} \mathbf{S}_k \times (\mathbf{S}_k \times \mathbf{H}_k)], \quad (20)$$

where γ_{es} is an electron-spin damping parameter, $\mathbf{H}_k = \sum_i J_{ik} \mathbf{S}_i$ is the effective exchange field acting on spin k , and \mathbf{h}_k is a δ -correlated fluctuating exchange field, satisfying the conditions $\langle \mathbf{h}_k \rangle = 0$ and $\langle h_{i\alpha}(t) h_{j\beta}(t') \rangle = \mu_{es} \delta_{ij} \delta_{\alpha\beta} \delta(t - t')$. We have noted in Ref. 9 that energy exchange between the lattice and spin subsystems involves terms in Eqs. (19) and (20) that depend on the derivative of the coordinate-dependent exchange coupling function $J_{ij}(\mathbf{R})$.

Similarly to the LE case treated above, we assume that the fluctuation and dissipation terms in Eqs. (19) and (20) result from the interaction with the electronic subsystem. The rates of energy change for the lattice and spin subsystems in region A are

$$\begin{aligned} \frac{dE_{l,A}}{dt} &= f_{l,A}(\mathbf{R}, \mathbf{p}) + g_{sl,A}(\mathbf{R}, \mathbf{p}, \mathbf{S}) \\ &\quad + \sum_{k \in A} \left(\frac{\mathbf{p}_k}{m} \cdot \mathbf{f}_k - \gamma_{el} \frac{\mathbf{p}_k^2}{m^2} \right), \end{aligned} \quad (21)$$

$$\begin{aligned} \frac{dE_{s,A}}{dt} &= f_{s,A}(\mathbf{S}) - g_{sl,A}(\mathbf{R}, \mathbf{p}, \mathbf{S}) \\ &\quad - \frac{1}{\hbar} \sum_{k \in A} [\mathbf{H}_k \cdot (\mathbf{S}_k \times \mathbf{h}_k) + \gamma_{es} |\mathbf{S}_k \times \mathbf{H}_k|^2], \end{aligned} \quad (22)$$

where

$$\begin{aligned} f_{s,A}(\mathbf{S}) &= \frac{\gamma_{es}}{2\hbar} \sum_{i \in A} |\mathbf{S}_i \times \mathbf{H}_i|^2 \\ &\quad - \frac{\gamma_{es}}{2\hbar} \sum_j \left[\mathbf{S}_j \times \left(\sum_{i \in A} J_{ij} \mathbf{S}_i \right) \cdot (\mathbf{S}_j \times \mathbf{H}_j) \right] \\ &\quad - \frac{1}{2\hbar} \sum_j \left[\left(\sum_{i \in A} J_{ij} \mathbf{S}_i \right) \cdot (\mathbf{S}_j \times \mathbf{H}_j) \right], \end{aligned} \quad (23)$$

$$g_{sl,A}(\mathbf{R}, \mathbf{p}, \mathbf{S}) = \frac{1}{2} \sum_{i \in A} \sum_{j,k} \left(\frac{\partial J_{ij}}{\partial \mathbf{R}_k} \cdot \frac{\mathbf{p}_k}{m} \right) (\mathbf{S}_i \cdot \mathbf{S}_j), \quad (24)$$

and $\mathbf{S} = \{\mathbf{S}_1, \mathbf{S}_2, \dots, \mathbf{S}_N\}$. Function $f_{s,A}(\mathbf{S})$ describes the flow of energy within the spin subsystem only, and its meaning is similar to that of function $f_{l,A}(\mathbf{R}, \mathbf{p})$ describing the lattice subsystem. The sum of functions $f_{s,A}(\mathbf{S})$ for all the regions is equal to zero, confirming the internal consistency of the above equations. Function $g_{sl,A}(\mathbf{R}, \mathbf{p}, \mathbf{S})$ describes energy exchange between the spin and lattice subsystems.

Taking the ensemble averages of (21) and (22), and applying the Furutsu-Novikov theorem^{53–57} to the terms containing fluctuating forces and fields, we arrive at

$$\begin{aligned} \frac{d\langle E_{l,A} \rangle}{dt} &= \langle f_{l,A} \rangle + \langle g_{sl,A} \rangle + \frac{3N\mu_{el}}{2m} \\ &\quad - \frac{3Nk_B T_l \gamma_{el}}{m}, \end{aligned} \quad (25)$$

$$\begin{aligned} \frac{d\langle E_{s,A} \rangle}{dt} &= \langle f_{s,A} \rangle - \langle g_{sl,A} \rangle + \frac{\mu_{es}}{\hbar^2} \sum_{k \in A} \langle \mathbf{S}_k \cdot \mathbf{H}_k \rangle \\ &\quad - \frac{\gamma_{es}}{\hbar} \sum_{k \in A} \langle |\mathbf{S}_k \times \mathbf{H}_k|^2 \rangle. \end{aligned} \quad (26)$$

Following the same mathematical line of derivation as in the LE case above, and assuming that the magnitudes of fluctuating forces and fluctuating exchange fields are proportional to the electronic temperature, we write the fluctuation-dissipation

relation for the lattice^{15–17} and the spins^{9,18,26,27} as $\mu_{el} = 2\gamma_{el}k_B T_e$ and $\mu_{es} = 2\hbar\gamma_{es}k_B T_e$, respectively. To proceed with the analysis, we now need an equation that would relate spin directions to the effective temperature of spins T_s . Such an equation was derived in Ref. 27. It has the form

$$T_s = \frac{\sum_k \langle |\mathbf{S}_k \times \mathbf{H}_k|^2 \rangle}{2k_B \sum_k \langle \mathbf{S}_k \cdot \mathbf{H}_k \rangle}. \quad (27)$$

Substituting the above equations into (25) and (26), we arrive at

$$\frac{d\langle E_{l,A} \rangle}{dt} = \langle f_{l,A} \rangle + \langle g_{sl,A} \rangle + \frac{3Nk_B\gamma_{el}}{m}(T_e - T_l), \quad (28)$$

$$\begin{aligned} \frac{d\langle E_{s,A} \rangle}{dt} &= \langle f_{s,A} \rangle - \langle g_{sl,A} \rangle \\ &+ \frac{2k_B\gamma_{es}}{\hbar} \sum_{k \in A} \langle \mathbf{S}_k \cdot \mathbf{H}_k \rangle (T_e - T_s). \end{aligned} \quad (29)$$

On the other hand, a phenomenological macroscopic 3TM³⁰ for the spin, lattice, and electron subsystems is described by a set of coupled heat transfer equations with heat diffusion terms, similar to those of the lattice-electron two-temperature model, namely

$$C_l \frac{dT_l}{dt} = \nabla(\kappa_l \nabla T_l) + G_{sl}(T_s - T_l) + G_{el}(T_e - T_l), \quad (30)$$

$$C_s \frac{dT_s}{dt} = \nabla(\kappa_s \nabla T_s) + G_{sl}(T_l - T_s) + G_{es}(T_e - T_s), \quad (31)$$

$$C_e \frac{dT_e}{dt} = \nabla(\kappa_e \nabla T_e) + G_{el}(T_l - T_e) + G_{es}(T_s - T_e). \quad (32)$$

Comparing equations (28) and (29) with (30) and (31) we arrive at the same expression for the electron-lattice heat transfer coefficient G_{el} as that found in the 2TM above. Also, we find the electron-spin heat transfer coefficient

$$G_{es} = \frac{2k_B\gamma_{es}}{\hbar V_A} \sum_{k \in A} \langle \mathbf{S}_k \cdot \mathbf{H}_k \rangle, \quad (33)$$

where V_A is the volume of region A . Although the ensemble average of function $\langle g_{sl,A} \rangle$ cannot at this point be mapped directly onto the term $G_{sl}(T_s - T_l)$, this does not impede the development of the spin-lattice-electron dynamics (SLED) model, which involves explicit integration of equations of motion for the atoms and spins.

It is interesting that G_{es} is not simply proportional to γ_{es} , as in the LE case. G_{es} also contains a term proportional to the local energy of the spin subsystem since

$$\sum_{k \in A} \langle \mathbf{S}_k \cdot \mathbf{H}_k \rangle = \sum_{k \in A} \sum_i \langle J_{ik}(\mathbf{R}) \mathbf{S}_k \cdot \mathbf{S}_i \rangle \quad (34)$$

$$= -2\langle E_{s,A} \rangle, \quad (35)$$

where $E_{s,A}$ is the total energy of interaction between the spins in region A .

In principle, this temperature-dependent quantity may be measured experimentally using neutron scattering.^{63,64} For example, assuming that the exchange parameters $J_{ij}(\mathbf{R})$ are appreciable only for the first and second nearest neighbor pairs of atoms in a bcc lattice, and that fluctuations of these parameters about their average values J_1 and J_2 are small, we can write

$$\langle \mathbf{S}_i \cdot \mathbf{H}_i \rangle \approx 8J_1 \langle \mathbf{S}_i \cdot \mathbf{S}_j \rangle_1 + 6J_2 \langle \mathbf{S}_i \cdot \mathbf{S}_j \rangle_2, \quad (36)$$

where $\langle \mathbf{S}_i \cdot \mathbf{S}_j \rangle_1$ and $\langle \mathbf{S}_i \cdot \mathbf{S}_j \rangle_2$ are the first and second nearest neighbor spin-spin correlation functions. These spin-spin correlation functions can be measured experimentally using neutron scattering.⁶⁴

The spin-lattice-electron dynamics (SLED) model is fully defined by Eqs. (18), (19), (20), and (32), where the heat transfer coefficients G_{el} and G_{es} are given by Eqs. (10) and (33). The local lattice temperature T_l and the local spin temperature T_s are evaluated using the equipartition principle and Eq. (27). The temperature of the electrons T_e is a spatially varying local quantity, the evolution of which is described by the heat transfer equation. Energy exchange between the spins and electrons, and between the lattice atoms and electrons, is described by the Langevin fluctuation and dissipation terms, whereas the exchange of energy between the spins and atoms in the lattice is described by the terms containing the coordinate-dependent exchange coupling function $J_{ij}(\mathbf{R})$ and its derivative entering Eqs. (19) and (20).

The SLED model formulated above describes a closed system. At the same time, the mathematical implementation of the model is such that in practical simulations the total energy fluctuates. This stems from the fact that we use two conceptually different, although statistically equivalent, approaches to the treatment of energy exchange between the lattice and spin degrees of freedom on the one hand, and electronic degrees of freedom on the other. In the equations of motion for the atoms and spins, interaction with the electronic subsystem is described by the Langevin fluctuating and dissipative forces and fields. At the same time, the effect of the lattice and the spins on the electrons is described by the deterministic coefficients G_{el} and G_{es} entering the heat transfer equations for the local temperature of the electrons. The two approaches match each other exactly in the limit where we consider ensemble average quantities. Bearing this in mind, in what follows we apply SLED to simulating the processes that evolve over sufficiently long intervals of time, where the cumulative effect of Langevin stochastic forces approaches its ensemble average limit, and where the energy exchange between different subsystems is equally well described by the stochastic Langevin and the deterministic heat transfer equations.

B. Parametrization of the damping constants and simulation of laser pulse demagnetization

In SLED, the interatomic potential⁶⁵ $U(\mathbf{R})$ and the exchange coupling function⁹ $J_{ij}(\mathbf{R})$ are deduced from either *ab initio* calculations or experimental data, and fitted to certain functional forms. At the same time, the values of damping parameters γ_{es} and γ_{el} , which determine the rates of electron-spin and electron-lattice relaxation time scales, remain largely unknown. In principle, these parameters may be calculated taking into account spin-orbit interactions^{37–39} and electron-atom scattering cross sections,¹¹ respectively. Alternatively, one could follow an arguably more direct and accurate approach, which does not require knowing the actual microscopic mechanism of energy transfer, and fit simulations directly to experimental data.

In laser-pulse demagnetization experiments on magnetic metals,^{30–37} the exposure of a thin magnetic film to a laser

pulse gives rise to a fast drop in magnetization occurring within the first picosecond, followed by the magnetization re-emerging over the next few picoseconds. The initial drop in magnetization is believed to come from the strong coupling between the electrons and spins, whereas the magnetization recovery appears to be a thermal equilibrium process.^{30,31} Carpena *et al.*³² found that the demagnetization and the remagnetization recovery time constants are of the order of 0.1 and 0.8 ps, respectively, for the case of iron thin films.

Within the 3TM³⁰ the hierarchy of energy relaxation processes is determined by the magnitudes of the heat transfer coefficients G_{es} , G_{el} , and G_{sl} . Since we have already established a relationship between the damping constants and the heat transfer coefficients, we expect that SLED simulations should be able to reproduce the behavior found in the 3TM.

We perform SLED simulations using a cell containing 54 000 atoms in bcc crystal structure. Simulations describe bcc ferromagnetic iron, and use the DDBN interatomic potential,^{65,66} with correction to the magnetic ground state energy noted in Ref. 9. Exchange coupling is approximated by a pairwise function of the distance between the atoms⁹ $J_{ij}(r_{ij}) = J_0(1 - r_{ij}/r_c)^3 \Theta(r_c - r_{ij})$, where $J_0 = 749.588$ meV, $r_c = 3.75$ Å, and Θ is the Heaviside step function. Here the magnitude of J_0 is different from that used in Ref. 9 to reflect the fact that here we use the atomic spin $\mathbf{S}_i = -\mathbf{M}_i/g\mu_B$ as a variable, where $M_i = 2.2\mu_B$ is the atomic magnetic moment and g is the electronic g factor. The functional form of the temperature-dependent electronic specific heat $C_e = 3 \tanh(2 \times 10^{-4} T_e) k_B$ (per atom) is adopted from Ref. 12.

After the initial thermalization of the simulation cell to 300 K, a Gaussian energy pulse with the standard deviation of 15 fs is introduced in the electronic subsystem, to mimic the effect of a 60 fs laser pulse used in experiments by Carpena *et al.*³² The probe pulse is not included in the simulations since the demagnetization process is solely induced by the pump pulse. The peak of the pump pulse is at $t = 0$ in Figs. 1 and 2. In simulations we neglect the diffusion term in the

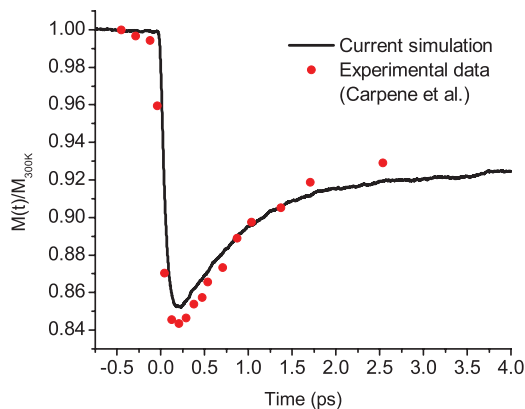


FIG. 1. (Color online) Evolution of magnetization as a function of time. The entire curve is normalized to the value of magnetization at 300 K. By tuning the damping constants and the amplitude of the energy pulse we match the simulated demagnetization process to experimental observations by Carpena *et al.*³² The simulated demagnetization curve was computed assuming $\gamma_{el}/m = 0.6$ ps⁻¹ and $\gamma_{es} = 8 \times 10^{-3}$ (the latter parameter is dimensionless).

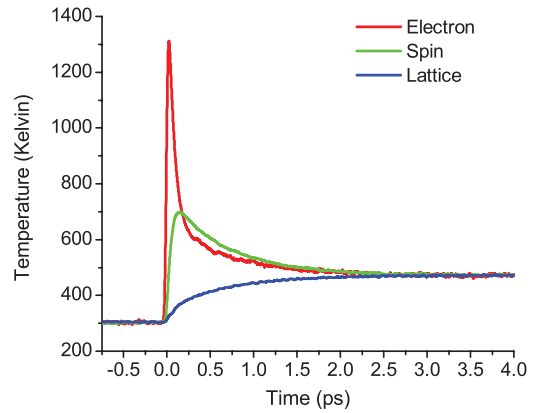


FIG. 2. (Color online) Evolution of temperatures for the spin, lattice, and electronic subsystems as functions of time. The electronic temperature rapidly increases initially due to the absorption of energy from the laser pulse, followed by the increase of the spin temperature. At some point, the spin temperature becomes higher than the temperature of the electrons. The temperature of the lattice increases much slower due to the weak electron-lattice coupling, and even weaker spin-lattice coupling.

electron heat transfer equation and assume that the electron temperature is spatially homogeneous.

Figure 1 shows magnetization as a function of time. The entire curve is normalized to the value of magnetization at 300 K. By tuning the damping constants and the amplitude of the energy pulse we match the simulated demagnetization process to experimental points taken from Ref. 32. The energy of the pulse determines the amplitude of variation of magnetization as a function of time, whereas the damping constants determine the relaxation time scales. Several simulations were performed assuming different energy of the pulse to find the best match to experimental observations. In experiment, the only parameter that characterizes the pulse the energy of pulse per unit *area* rather than per unit *volume*. This leaves a fraction of the pulse energy transferred to the electron subsystem not fully defined. In the simulations, to match observations, we adjusted the pulse energy to match both the depth of the trough in the observed magnetization curve and its equilibrium value. The experimental data are well reproduced if we assume that $\gamma_{el}/m = 0.6$ ps⁻¹ and $\gamma_{es} = 8 \times 10^{-3}$ (the latter parameter is dimensionless).

Figure 2 shows the time evolution of temperatures for the spin, lattice, and electronic subsystems. The overall shape of the curves is very similar to that found for Ni using the 3TM,³⁰ and for Ni and Gd using a microscopic 3TM model.³¹ The electronic temperature rapidly increases initially due to the absorption of energy from the laser pulse, followed by the increase of the spin temperature. At some point, the spin temperature becomes higher than the temperature of the electrons. It is due to the absorption of energy from electrons to the lattice subsystem, where the temperature of the lattice increases much slower due to the weak electron-lattice coupling, and even weaker spin-lattice coupling. The change of temperatures during this transient state is the result of an interplay of between various relaxation and equilibration processes involving all the three subsystems.

Comparing Figs. 1 and 2 we see that the origin of fast demagnetization observed in laser experiments on thin films is associated with strong electron-spin coupling, where spins initially absorb energy from the electrons, followed by the relatively slow recovery toward thermal equilibrium. The fact that it appears possible to accurately fit the experimental demagnetization curves not only confirms the validity of the SLED model, but also suggests that the numerical values of dissipative parameters derived from fitting simulations to experimental data can be used in other applications, for example, in simulations of collision cascades or propagation of a shock wave through a magnetic metal.

IV. COLLECTIVE MOTION OF ELECTRONS AND ATOMS

A. Modified Langevin equations of motion and the Fokker-Planck equation

If a group of atoms moves uniformly in the same direction as a single entity, the formula $T_i = 2/(3Nk_B) \sum_i \mathbf{p}_i^2/2m$ for the kinetic temperature does not apply. Although this statement is almost self-evident—indeed in the case of uniform collective motion the distribution of velocities of atoms is so different from the Maxwell distribution that it does not even satisfy the condition $\langle \mathbf{p}_i \rangle = \overline{\mathbf{p}_i(t)} = 0$ —it is not immediately obvious how to separate the local collective motion of atoms, often observed in large-scale simulations, from their random thermal motion.

If we assume that a particular system is in thermal equilibrium in its moving center of mass frame, then its temperature is defined as $T_i = 2/(3Nk_B) \sum_i (\mathbf{p}_i - \mathbf{P})^2/2m$, where $\mathbf{P} = 1/N \sum_i \mathbf{p}_i$ is the average momentum of atoms. Similarly, the average momentum needs to be subtracted from the instantaneous momentum of each atom in order to evaluate the local temperature of the lattice, if the uniform motion of atoms occurs locally, for example, in simulations of shock waves described below.

In the LED and SLED models, the electronic subsystem is coupled to the lattice and spin subsystems through the heat transfer equation for the temperature of the electrons. The temperature of the electrons is defined assuming that there is no uniform, or local collective, motion of atoms in the material. Adopting such an approximation results in the overestimation of the rate of dissipation of energy of atoms to the electrons if the simulations show the occurrence of local collective motion. For example, local collective motion is observed in simulations of high-energy collision cascades where atomic displacements occur as shock waves propagating away from the point of initial impact.⁴³ Since the dissipation of energy from the lattice to electrons heats up the electronic subsystem and enhances defect annealing,¹² it is desirable to avoid overestimating the lattice energy dissipation and the resulting uncertainties in the defect production rates.

One possible way of including the effect of correlated motion of atoms and electrons in the treatment of energy losses consists of replacing the heat transfer equation for the electrons with the Navier-Stokes equations.⁶⁷ Another way, which we adopt below, is to treat the lattice-electron energy transfer in the moving frame, associated with the local atomic subsystem. This approach relies on the “nearsightedness” of electronic

structure,^{68,69} where interatomic bonding and other forms of atom-electron interactions are local properties of the material, and where the dynamics of energy losses is primarily sensitive to the local environment of a given atom. To take advantage of the nearsightedness of electronic structure, we rewrite Eqs. (3) and (4) as follows:

$$\frac{d\mathbf{R}_i}{dt} = \frac{\mathbf{p}_i}{m}, \quad (37)$$

$$\frac{d\mathbf{p}_i}{dt} = -\frac{\partial U}{\partial \mathbf{R}_i} - \frac{\gamma_{el}}{m}(\mathbf{p}_i - \mathbf{p}_A) + (\mathbf{f}_i - \mathbf{f}_A), \quad (38)$$

where

$$\mathbf{p}_A = \frac{1}{N_A} \sum_{i \in A} \mathbf{p}_i, \quad (39)$$

$$\mathbf{f}_A = \frac{1}{N_A} \sum_{i \in A} \mathbf{f}_i. \quad (40)$$

Here index A refers to a local region of the atomic subsystem defined the same way as in the treatment of lattice-electron dynamics above. In this way the average dissipation and fluctuation forces are eliminated from the equations of motion for the atoms. The change of the average momentum of atoms in region A with respect to time is

$$\frac{d\mathbf{p}_A}{dt} = \frac{1}{N_A} \sum_{i \in A} \left(-\frac{\partial U}{\partial \mathbf{R}_i} \right), \quad (41)$$

and it is not affected by dissipation and fluctuations. The above equations can be interpreted as describing the local collective motion of atoms *and* electrons. This collective motion is nondissipative since it does not generate dynamic friction resulting from the relative motion of atoms with respect to electrons. On the other hand, in the locally moving frame the temperatures of atoms and electrons may differ and hence equilibration will occur according to the same dissipative laws as in the spatially homogeneous nonequilibrium case.

To derive the fluctuation-dissipation relation we use Eqs. (37) and (38) and map them onto the Fokker-Planck equation^{18,27,70,71}

$$\frac{\partial W}{\partial t} = -\sum_{\Theta} \frac{\partial}{\partial x_{\Theta}} (A_{\Theta} W) + \frac{1}{2} \sum_{\Theta, \Phi} \frac{\partial^2}{\partial x_{\Theta} \partial x_{\Phi}} (B_{\Theta\Phi} W), \quad (42)$$

where $\mathbf{x} = \{\mathbf{R}, \mathbf{p}\} = \{\mathbf{R}_1, \mathbf{R}_2, \dots, \mathbf{R}_N, \mathbf{p}_1, \mathbf{p}_2, \dots, \mathbf{p}_N\}$, indexes Θ and Φ refer to the Cartesian components of coordinates and momenta, $A_{\Theta} = \lim_{\Delta t \rightarrow 0} \frac{1}{\Delta t} \langle x_{\Theta} \rangle$ is the drift coefficient, and $B_{\Theta\Phi} = \lim_{\Delta t \rightarrow 0} \frac{1}{\Delta t} \langle x_{\Theta} x_{\Phi} \rangle$ is the diffusion coefficient.

The drift and diffusion coefficients for the coordinates and momenta have the form^{18,27,70,71}

$$\mathbf{A}_i^R = \frac{\mathbf{p}_i}{m}, \quad (43)$$

$$\mathbf{A}_i^P = -\frac{\partial U}{\partial \mathbf{R}_i} - \frac{\gamma_{el}}{m}(\mathbf{p}_i - \mathbf{p}_A), \quad (44)$$

$$B_{i\alpha i\alpha}^R = B_{i\alpha i\beta}^R = B_{i\alpha j\alpha}^R = B_{i\alpha j\beta}^R = 0, \quad (45)$$

$$B_{i\alpha i\beta}^P = B_{i\alpha j\beta}^P = 0, \quad (46)$$

$$B_{i\alpha i\alpha}^p = \mu_{el} \left(1 - \frac{1}{N_A}\right), \quad (47)$$

$$B_{i\alpha j\alpha}^p = \begin{cases} -\mu_{el}/N_A & \text{if } i \text{ and } j \in \text{region } A \\ 0 & \text{if } i \text{ or } j \notin \text{region } A. \end{cases} \quad (48)$$

In the thermal equilibrium limit the energy distribution approaches the Gibbs distribution $W = W_0 \exp(-E_l/k_B T)$, where W_0 is a normalization constant. Substituting this distribution into the Fokker-Planck equation, we find

$$\frac{\partial W}{\partial t} = \left(\frac{\mu_{el}}{2k_B T} - \gamma_{el} \right) \times \left\{ \sum_i \left[\frac{\mathbf{p}_i^2 - \mathbf{p}_A^2}{mk_B T} - 3 \left(1 - \frac{1}{N_A}\right) \right] \right\} W. \quad (49)$$

At equilibrium $\partial W/\partial t = 0$. In this limit the right-hand side of Eq. (49) vanishes if at least one of the following conditions is satisfied, namely

$$\mu_{el} = 2\gamma_{el}k_B T, \quad (50)$$

which is the original fluctuation-dissipation relation, or

$$\frac{1}{m} \sum_i (\mathbf{p}_i^2 - \mathbf{p}_A^2) = 3k_B T \sum_i \left(1 - \frac{1}{N_A}\right), \quad (51)$$

which is a modified equipartition relation. Adopting Eq. (51) is equivalent to averaging over the Gibbs distribution. In what follows we assume that this relation applies to every local region in the system, namely

$$\frac{1}{m} \left(\sum_{i \in A} \mathbf{p}_i^2 - N_A \mathbf{p}_A^2 \right) = 3k_B T (N_A - 1). \quad (52)$$

We now repeat the procedure of relating the equations of motion of atoms to the heat transfer equation. The rate of energy change for region A is

$$\begin{aligned} \frac{dE_{l,A}}{dt} &= f_{l,A}(\mathbf{R}, \mathbf{p}) + \sum_{i \in A} \frac{\mathbf{p}_i}{m} \cdot (\mathbf{f}_i - \mathbf{f}_A) \\ &\quad - \frac{\gamma_{el}}{m^2} \left(\sum_{i \in A} \mathbf{p}_i^2 - N_A \mathbf{p}_A^2 \right). \end{aligned} \quad (53)$$

Taking the ensemble average of Eq. (53), and applying Eq. (52) together with the Furutsu-Novikov theorem,^{53–57} we find that

$$\frac{d\langle E_{l,A} \rangle}{dt} = \langle f_{l,A} \rangle + \frac{3(N_A - 1)\mu_{el}}{2m} - \frac{3(N_A - 1)\gamma_{el}k_B T_l}{m}. \quad (54)$$

Substituting equation $\mu_{el} = 2\gamma_{el}k_B T_e$ into Eq. (54), we arrive at

$$\frac{d\langle E_{l,A} \rangle}{dt} = \langle f_{l,A} \rangle + \frac{3(N_A - 1)\gamma_{el}k_B}{m} (T_e - T_l). \quad (55)$$

The heat transfer coefficients, describing also the effect of local collective motion of atoms, can now be found by comparing Eq. (55) with (14), namely

$$G_{el} = \frac{3(N_A - 1)\gamma_{el}k_B}{mV_A}. \quad (56)$$

There is no heat transfer between the atoms and electrons in the limit where $N_A = 1$.

The same line of derivation applies to the SLED model, which can now be used for treating spatially homogeneous system as well as a system exhibiting local collective motion of atoms.

B. Examples of practical simulations

In this section we describe simulations of compressive elastic waves propagating in ferromagnetic iron. The simulations are carried out using the SLED model with and without the local collective motion of atoms approximation. Pure MD simulations are also performed for comparison. Simulation cells contain $30 \times 30 \times 550$ body-centered cubic (bcc) unit cells with the coordinate axes parallel to the [100], [010], and [001] crystallographic directions, and involve the total of 990 000 atoms and spins. The damping parameters γ_{es} and γ_{el} used in the simulations are assigned values derived from experimental data on laser-induced demagnetization of iron thin films. The heat transfer equation also includes the diffusion term with $\kappa_e = 80 \text{ W m}^{-1} \text{ K}^{-1}$, which is assumed to be temperature independent. The samples are initially thermalized to 300 K.

The local regions needed for identifying the velocities of local collective motion of atoms are defined using the linked cells algorithm that provides an intrinsic *finite difference* grid naturally present in MD and SLD simulations. Each linked cell is assigned a unique set of values T_s , T_l , and T_e that are recalculated at each time step. The coupled equations of motion for the spins and lattice, and the heat transfer equation for the electrons, are integrated using an algorithm^{26,41} based on the Suzuki-Trotter decomposition.^{72–76} Its symplectic nature guarantees the accumulation of very small numerical error, which is a condition required for the accurate computation of the energy exchange rates. The integration time step is 1 fs, which is approximately one tenth of the inverse Larmor frequency for the precession of spins.

Two compressive waves propagating in the opposite directions are generated using a method proposed by Holian *et al.*,^{77,78} where a simulation box with periodic boundary conditions is shrunk uniaxially, introducing symmetric impacts on both sides of the box. The boundaries on the left and right move inwards with velocity u_p , and this is equivalent to applying the action of two pistons moving with velocity u_p in the [001] and [00 $\bar{1}$] directions (Fig. 3). In our simulations, artificial compression is applied for 0.5 ps, with $u_p = 500 \text{ m/s}$. After the initial transformation, the cell size and shape are kept constant. Two elastic compressive shock waves, both propagating toward the center of the cell, form as a result of the initial transformation. The relatively small lateral size of the cell in the directions perpendicular to the direction of propagation of the shock waves is the reason why plastic deformation, observed in other shock wave simulations,⁴² did not occur in our case.

Figure 4 shows profiles of local temperatures T_s , T_l , and T_e simulated using SLED, and profiles of T_l simulated using pure MD, following the initiation of the shock waves. The simulations illustrated in Fig. 4 did not consider collective motion of atoms and electrons. Each temperature point in

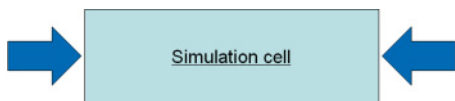


FIG. 3. (Color online) Schematic representation of simulation setup. A simulation cell contains $30 \times 30 \times 550$ body-centered cubic (bcc) unit cells, or approximately $86 \text{ \AA} \times 86 \text{ \AA} \times 1577 \text{ \AA}$, with the coordinate axes parallel to the $[100]$, $[010]$, and $[001]$ crystallographic directions, and involves the total of 990 000 atoms and spins. Two compressive waves propagating in the opposite directions are generated by using a method proposed by Holian *et al.*,^{77,78} where a simulation box with periodic boundary conditions is shrunk uniaxially, introducing symmetric impacts on both sides of the box. The boundaries on the left and on the right move inwards with velocity $u_p = 500 \text{ m/s}$. This is equivalent to applying the action of two pistons moving with velocity u_p in the $[001]$ and $[00\bar{1}]$ directions. Artificial compression is applied for 0.5 ps.

the figures corresponds to the average temperature of atoms in a linked cell situated at a given coordinate point in the direction of propagation of a shock wave. Since the effect of local collective motion is not included here, the lattice temperature T_l is proportional to the kinetic energy of atoms

defined in the frame associated with the static boundaries of the simulation cell. The position of the compressive wave front corresponds to the peak of T_l . In comparison with a pure MD simulation, in the SLED case the energy of atoms is rapidly absorbed by the spin and electron subsystems. The rate of attenuation of the shock waves is much higher in the SLED model than in MD simulations. In SLED the energy of moving atoms is transferred into the electron subsystem via the dissipative Langevin term. The energy of the electrons is then rapidly transferred to the spin subsystem. In comparison, in MD simulations the only mode of dissipation is associated with anharmonic phonon-phonon interactions, and the energy dissipation rate is much lower than in the SLED model.

However, if the local collective motion of atoms is taken into consideration, then the predicted rate of dissipation of energy from the moving atoms to the electrons differs significantly from that found in simulations shown in Fig. 4. First of all, the lattice temperature T_l shown in Fig. 5 and calculated using Eq. (52), is significantly lower than that shown in Fig. 4, confirming the fact that the kinetic energy of local collective motion of atoms is not related to the local temperature. We can still see the propagating wave front, but the temperature

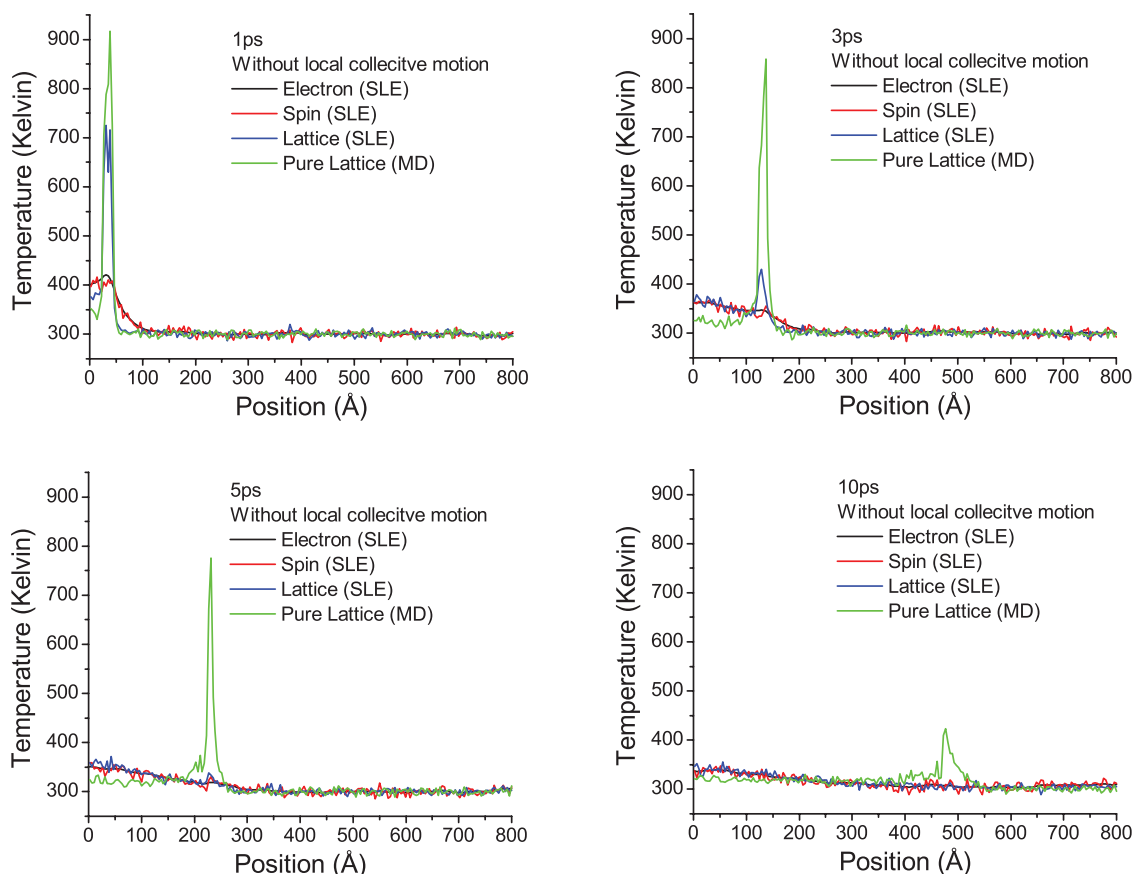


FIG. 4. (Color online) Profiles of local temperatures T_s , T_l , and T_e simulated using SLED, and profiles of T_l simulated using pure MD, following the initiation of the shock waves. No consideration of the local collective motion of atoms and electrons is included in these simulations. Each temperature point in the figures corresponds to the average temperature of atoms in a linked cell situated at a given coordinate point in the direction of propagation of a shock wave. The lattice temperature T_l is proportional to the kinetic energy of atoms defined in the frame associated with the static boundaries of the simulation cell. The position of the compressive wave front corresponds to the peak of T_l . In comparison with a pure MD simulation, in the SLED case the energy of atoms is rapidly absorbed by the spin and electron subsystems, resulting in the much higher rate of attenuation of the compressive wave predicted by the SLED model in comparison with pure MD simulations.

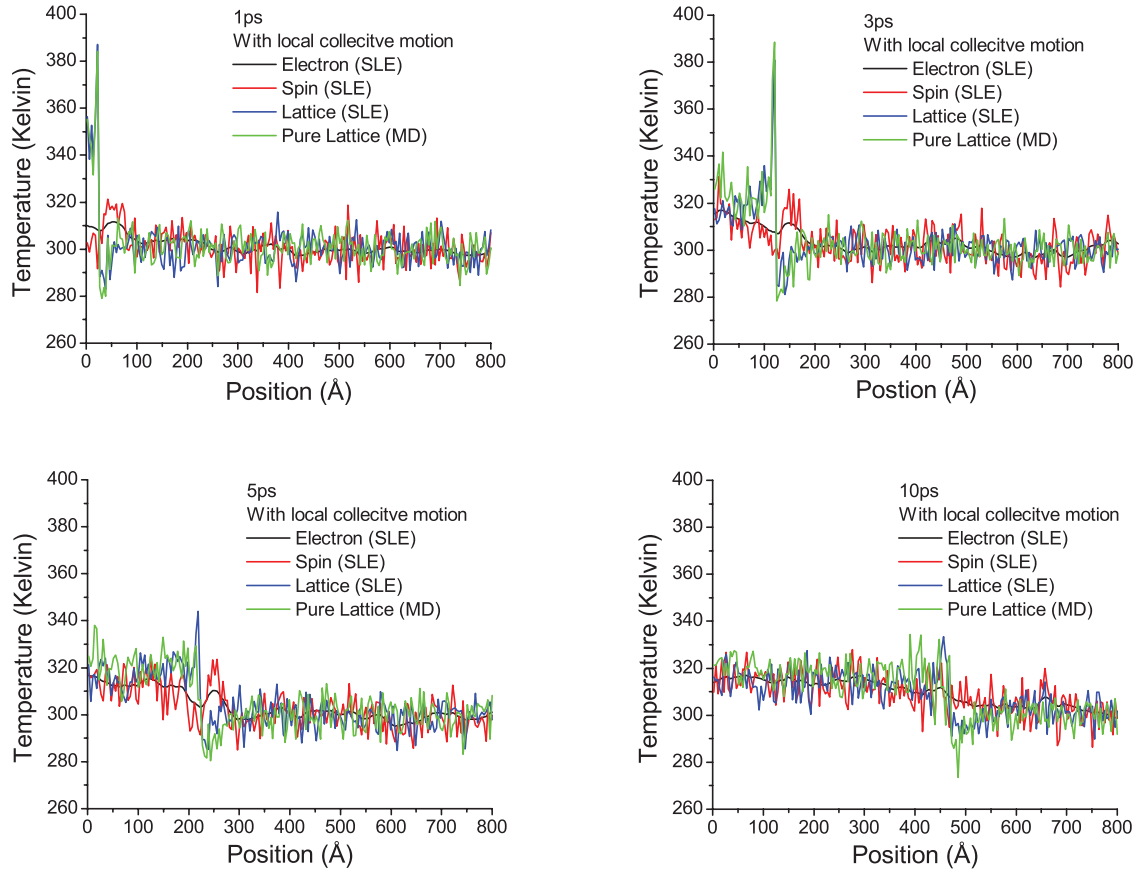


FIG. 5. (Color online) Profiles of local temperatures T_s , T_l , and T_e simulated using SLED, and profiles of T_l simulated using pure MD, following the initiation of the shock waves. Local collective motion is taken into account in the simulations. The lattice temperature T_l calculated using Eq. (52) is significantly lower than that shown in Fig. 4. We can still see the propagating wave front, but the temperature profile predicted by the SLED model now closely resembles the temperature profile found in MD simulations.

profile predicted by the SLED model now closely resembles the temperature profile found in MD simulations. Examining the average velocity distributions evaluated for cases where local collective motion of atoms is/is not taken into account (see Fig. 6) we see that the predictions derived from the SLED model, which takes into account local collective motion of atoms, are very similar to those found in MD simulations. The rate of energy losses from the lattice to electrons predicted by SLED simulations is clearly excessive if local collective modes of motion of atoms occurring as a result of propagation of a shock wave are included in the definition of lattice temperature.

In both the SLED and MD simulations the compressive waves move at a constant velocity $u_s \approx 4500$ m/s, similar to the velocity of a longitudinal sound wave propagating through a single crystal of iron in the [001] direction,⁷⁹ where $c_{[001]} = \sqrt{C_{11}/\rho} \approx 5300$ m/s. This speed is not influenced by whether or not the effect of collective motion of atoms and electrons is taken into account in the treatment of energy dissipation.

The simulations described above show no spontaneous plastic deformation of the material occurring at the shock wave front, and only serve as examples proving the feasibility of the simulation method and consistency of the mathematical algorithm. Whether the propagation of a shock wave involving plastic deformation, generation of defects, and transfer of energy from the lattice to the electrons and spins occurring

in a large-scale simulation is going to follow a pattern similar to that shown in Figs. 4, 5, and 6, remains an open question and requires further analysis.

All the simulations described in this work were performed using GPU Nvidia GTX480 cards. In the case of SLED, the computational cost is about 2.5 times higher compared to a conventional MD simulation. It takes approximately 12.5 h to simulate the propagation of a shock wave over the interval of time of 10 ps.

V. DISSIPATIVE SPIN-LATTICE COUPLING

A. Spin fluctuations and spin-lattice energy transfer

The SLED model developed above did not explicitly consider the question about how energy is transferred between the spin and lattice subsystems since both subsystems were treated dynamically using the coupled SLD equations of motion for atoms and spins.⁹ This is different from the problem of energy exchange between the lattice and electrons, and between spins and electrons, where the treatment was based on the Langevin equations for atoms and spins, and on a heat transfer equation for the electrons, and where the determination of numerical values of damping parameters required a separate investigation and comparison of results of simulations to experimental observations. For completeness,

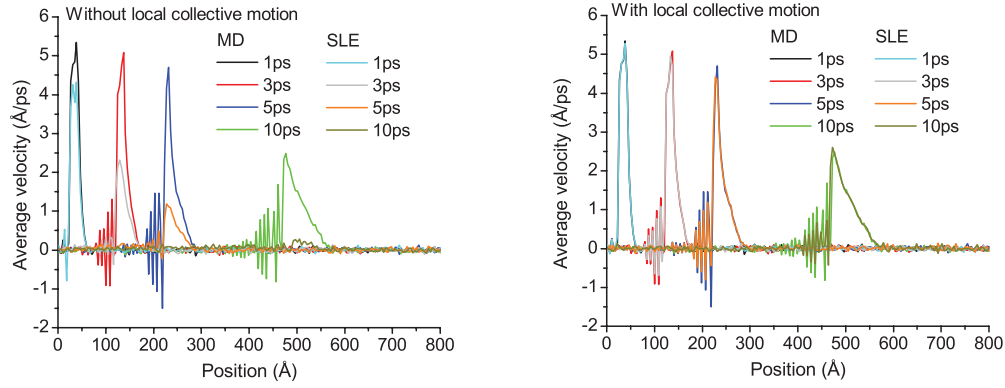


FIG. 6. (Color online) The average velocity distributions evaluated for cases where the local collective motion of atoms is/is not taken into account. Predictions derived from the SLED model that takes into account the local collective motion of atoms are very similar to those found in MD simulations. The rate of energy losses from the lattice to electrons found in SLED simulations is clearly excessive if the local collective modes of motion of atoms occurring as a result of propagation of a shock wave are included in the definition of lattice temperature.

here we explore if the energy transfer between the lattice and spins can be treated using a formalism broadly similar to that applied above to the treatment of interaction between the atoms and electrons, and spins and electrons.

The evolution of coupled lattice and spin systems is described by the spin-lattice dynamics equations⁹

$$\frac{d\mathbf{R}_k}{dt} = \frac{\mathbf{p}_k}{m}, \quad (57)$$

$$\frac{d\mathbf{p}_k}{dt} = -\frac{\partial U}{\partial \mathbf{R}_k} + \frac{1}{2} \sum_{i,j} \frac{\partial J_{ij}}{\partial \mathbf{R}_k} \mathbf{S}_i(t) \cdot \mathbf{S}_j(t), \quad (58)$$

$$\frac{d\mathbf{S}_k}{dt} = \frac{1}{\hbar} \left[\mathbf{S}_k \times \left(\sum_i J_{ik} \mathbf{S}_i \right) \right]. \quad (59)$$

These equations show how energy is transferred, on the microscopic level, from the spins to the lattice and vice versa. The momenta of the atoms, according to Eq. (58), evolve under the action of conservative interatomic forces described by the term $-\partial U/\partial \mathbf{R}_k$, and time-dependent rapidly fluctuating spin-orientation-dependent forces described by the second term in Eq. (58). If we average Eq. (58) over an interval of time inversely proportional to the Larmor frequency characterizing the time scale of spin precession, then the resulting equation will describe the slow adiabatic dynamics of atoms in the equally slowly varying external potential field of the form

$$\tilde{U}(\mathbf{R}) = U(\mathbf{R}) - \frac{1}{2} \sum_{i,j} J_{ij}(\mathbf{R}) \overline{\mathbf{S}_i(t) \cdot \mathbf{S}_j(t)}. \quad (60)$$

Assuming ergodicity, we replace the time averaged values by the ensemble averaged values. The rapidly fluctuating component of the force acting on atoms and resulting from the precession of spins is therefore

$$\mathbf{f}_k(t) = \frac{1}{2} \sum_{i,j} \frac{\partial J_{ij}}{\partial \mathbf{R}_k} [\mathbf{S}_i(t) \cdot \mathbf{S}_j(t) - \langle \mathbf{S}_i(t) \cdot \mathbf{S}_j(t) \rangle]. \quad (61)$$

This treatment follows the same logic as the one applied in Ref. 80 to the analysis of interactions between a mobile interstitial defect and thermal phonons.

Assuming that the statistics of fluctuating spin forces is not dissimilar to the statistics of fluctuations of Langevin forces acting on atoms, that is, that the forces become uncorrelated over an interval of time much shorter than the characteristic time scale of atomic motion, we write

$$\langle \mathbf{f}_k(t) \cdot \mathbf{f}_k(t') \rangle = 3\mu_{sl} \delta(t - t'), \quad (62)$$

where $\mu_{sl} = 2\gamma_{sl}k_B T$. This equation in fact defines the damping parameter γ_{sl} , the magnitude of which is related to the macroscopic rate of energy transfer between the spin and lattice subsystems, in the same way as the magnitude of parameter γ_{el} entering Eq. (4) is related to the electron-lattice heat transfer coefficient (10). To evaluate γ_{sl} we need to compute the integral of the four-point time-dependent spin correlation function

$$\begin{aligned} 6\gamma_{sl}k_B T &= \int_{-\infty}^{\infty} d(t-t') \langle \mathbf{f}_k(t) \cdot \mathbf{f}_k(t') \rangle \\ &= \frac{1}{4} \sum_{i,j} \frac{\partial J_{ij}}{\partial \mathbf{R}_k} \sum_{l,m} \frac{\partial J_{lm}}{\partial \mathbf{R}_k} \\ &\quad \times \int_{-\infty}^{\infty} d(t-t') \{ \langle [\mathbf{S}_i(t) \cdot \mathbf{S}_j(t)] [\mathbf{S}_l(t') \cdot \mathbf{S}_m(t')] \rangle \\ &\quad - \langle \mathbf{S}_i(t) \cdot \mathbf{S}_j(t) \rangle \langle \mathbf{S}_l(t') \cdot \mathbf{S}_m(t') \rangle \}. \end{aligned} \quad (63)$$

Assuming that the exchange coupling function is pairwise $J_{ij} = J_{ij}(|\mathbf{R}_i - \mathbf{R}_j|)$, we write

$$\frac{\partial J_{ij}}{\partial \mathbf{R}_k} = \left(\frac{\partial J_{ij}}{\partial R_{ij}} \right) \left(\delta_{ki} \frac{\mathbf{R}_k - \mathbf{R}_j}{|\mathbf{R}_k - \mathbf{R}_j|} + \delta_{kj} \frac{\mathbf{R}_k - \mathbf{R}_i}{|\mathbf{R}_k - \mathbf{R}_i|} \right). \quad (64)$$

Furthermore, taking that the derivative $J' = \partial J_{ij}/\partial R_{ij}$ remains constant over the interval of interatomic distances spanning the first and the second nearest neighbor atoms in bcc lattice, we write the fluctuating spin force acting on atom k as

$$\mathbf{f}_k(t) = J' \sum_{\mathbf{a}} \frac{\mathbf{a}}{|\mathbf{a}|} [\mathbf{S}_{\mathbf{a}}(t) \cdot \mathbf{S}_0(t) - \langle \mathbf{S}_{\mathbf{a}}(t) \cdot \mathbf{S}_0(t) \rangle], \quad (65)$$

where summation is performed over the nearest neighbor atoms. Using Eq. (65) we find an expression for γ_{sl} ,

$$\begin{aligned} \gamma_{sl} = & \frac{(J')^2}{6k_B T} \sum_{\mathbf{a}, \mathbf{b}} \frac{\mathbf{a} \cdot \mathbf{b}}{|\mathbf{a}||\mathbf{b}|} \int_{-\infty}^{\infty} d(t-t') \\ & \times \{ [\langle \mathbf{S}_{\mathbf{a}}(t) \cdot \mathbf{S}_0(t) \rangle [\langle \mathbf{S}_{\mathbf{b}}(t') \cdot \mathbf{S}_0(t') \rangle] \\ & - \langle \mathbf{S}_{\mathbf{a}}(t) \cdot \mathbf{S}_0(t) \rangle \langle \mathbf{S}_{\mathbf{b}}(t') \cdot \mathbf{S}_0(t') \rangle \}. \end{aligned} \quad (66)$$

Using the magnon expansion⁶³

$$\begin{aligned} \hat{S}_l^x &= \sqrt{\frac{S}{2}} (\hat{a}_l^\dagger + \hat{a}_l), & \hat{S}_l^y &= i\sqrt{\frac{S}{2}} (\hat{a}_l^\dagger - \hat{a}_l), \\ \hat{S}_l^z &= S - \hat{a}_l^\dagger \hat{a}_l, \\ \hat{\mathbf{S}}_l \cdot \hat{\mathbf{S}}_0 &= S(\hat{a}_l^\dagger \hat{a}_0^\dagger + \hat{a}_l^\dagger \hat{a}_0 - \hat{a}_l^\dagger \hat{a}_l - \hat{a}_0^\dagger \hat{a}_0), \end{aligned} \quad (67)$$

the Fourier representations of operators

$$\begin{aligned} \hat{a}_{\mathbf{R}}(t) &= \frac{1}{\sqrt{N}} \sum_{\mathbf{q}} \hat{a}_{\mathbf{q}} \exp(i\mathbf{q} \cdot \mathbf{R} - i\omega_{\mathbf{q}} t), \\ \hat{a}_{\mathbf{R}}^\dagger(t) &= \frac{1}{\sqrt{N}} \sum_{\mathbf{q}} \hat{a}_{\mathbf{q}}^\dagger \exp(-i\mathbf{q} \cdot \mathbf{R} + i\omega_{\mathbf{q}} t), \end{aligned} \quad (68)$$

and considering the classical limit, where the expectation values of operators are treated as quantities independent of their order, we arrive at an explicit formula for the spin-lattice damping parameter γ_{sl} ,

$$\begin{aligned} \gamma_{sl} = & \frac{(J')^2 \Omega^2}{6k_B T} \sum_{\mathbf{a}, \mathbf{b}} \frac{\mathbf{a} \cdot \mathbf{b}}{|\mathbf{a}||\mathbf{b}|} \int \frac{d^3 q d^3 k}{(2\pi)^5} n_{\mathbf{q}} n_{\mathbf{k}} \delta(\omega_{\mathbf{q}} - \omega_{\mathbf{k}}) \\ & \times [\exp(i\mathbf{k} \cdot \mathbf{a}) - 1][\exp(-i\mathbf{q} \cdot \mathbf{a}) - 1] \\ & \times [\exp(i\mathbf{q} \cdot \mathbf{b}) - 1][\exp(-i\mathbf{k} \cdot \mathbf{b}) - 1]. \end{aligned} \quad (69)$$

In this approximation the magnon frequency is⁶³

$$\omega_{\mathbf{q}} = \frac{S}{\hbar} \sum_{\mathbf{a}} J(|\mathbf{a}|) [1 - \cos(\mathbf{q} \cdot \mathbf{a})] \approx \frac{S}{2\hbar} \sum_{\mathbf{a}} J(|\mathbf{a}|) (\mathbf{q} \cdot \mathbf{a})^2, \quad (70)$$

where the last term describes the long wavelength limit, and the average magnon occupation numbers are

$$n_{\mathbf{q}} \approx \frac{k_B T}{\hbar \omega_{\mathbf{q}}}. \quad (71)$$

For bcc lattice, from (70) we find

$$\hbar \omega_{\mathbf{q}} = S a^2 \mathbf{q}^2 (J_1 + J_2), \quad (72)$$

where a is the lattice parameter and J_1 and J_2 are the exchange parameters for the first and second nearest neighbor coordination shells. Substituting Eqs. (71) and (72) into (69), and carrying out the integration, we find that γ_{sl} is a linear function of temperature T ,

$$\gamma_{sl} \approx \frac{7}{144} \left(\frac{12}{\pi} \right)^{1/3} \frac{\hbar (J')^2}{S} \frac{k_B T}{(J_1 + J_2)^3}. \quad (73)$$

Using the values $J' = -11.7957$ meV/Å, $J_1 = 22.52$ meV, $J_2 = 17.99$ meV, we find that to a good approximation $\gamma_{sl} \approx 0.8 \times 10^{-20} T$ eV s/Å², where temperature T is expressed in Kelvin units.

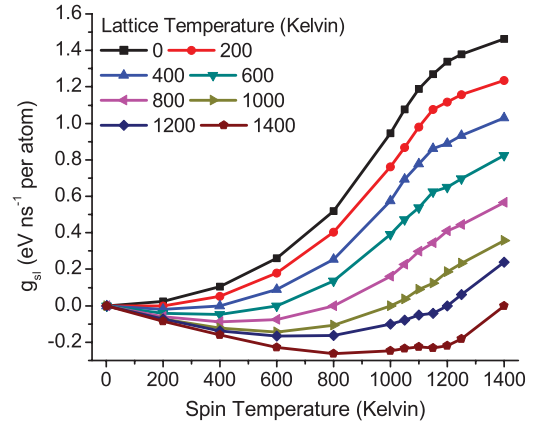


FIG. 7. (Color online) The spin-lattice energy transfer rate g_{sl} plotted as a function of the spin and lattice temperatures. The rate is calculated directly by using Eq. (24). The spin and lattice subsystems were kept at two different temperatures maintained using two independent Langevin thermostats. This makes it possible to calculate the cumulative amount of energy transferred from the spins to the lattice, or vice versa, for the case where the two subsystems are maintained at two different temperatures.

B. Spin-lattice energy transfer: Numerical simulations

To investigate the dynamics of spin-lattice energy transfer numerically, we use simulation cells containing 16 000 atoms and spins. To allow direct comparison with analytical results, we approximated the exchange coupling function by a linear expression $J_{ij} = J' R_{ij} + C$, with cutoff at 3.75 Å, where the numerical values of parameters J' and C were determined using a method developed by Schilfgaard *et al.*,⁶⁰ in which the linear muffin-tin orbital method is combined with Green's function technique. We calculated the values of J_{ij} for iron, using generalized gradient approximation,⁸¹ at the first and second nearest neighbor distances and find $J_1 = 22.52$ meV and $J_2 = 17.99$ meV. The values of parameters determined in this way are $J' = -11.7957$ meV/Å, and $C = 51.8024$ meV. These are the values that we used for analytical estimates given above. In dynamic simulations we used the Chiesa09⁸² interatomic potential.

We calculated the spin-lattice energy transfer rate g_{sl} directly by using Eq. (24), assuming that the spin and lattice temperatures were spatially homogeneous. The spin and the lattice subsystems were kept at two different temperatures maintained using two independent Langevin thermostats. This makes it possible to calculate the cumulative amount of energy transferred from the spins to the lattice, or vice versa, for the case where the two subsystems are maintained at two different temperatures. The data were accumulated over a 1 ns time interval once both the spin and lattice subsystem had been fully equilibrated at their respective temperatures. In the case where the temperature of the spins was close to the Curie temperature, very long equilibration times were used in the simulations.

Figure 7 shows the spin-lattice heat transfer rate g_{sl} plotted as a function of spin and lattice temperatures. It is interesting that there is no heat transfer between the two systems at $T_s = 0$, in agreement with Eq. (73). This is a consequence of the fact that no energy can be transferred to the spin subsystem if

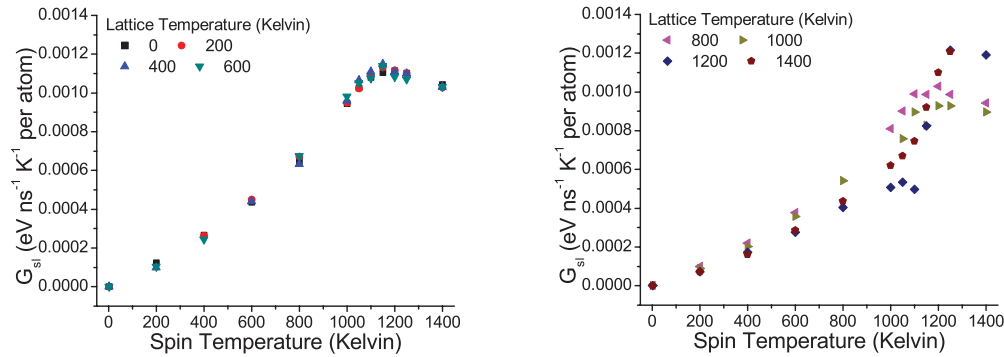


FIG. 8. (Color online) The spin-lattice heat transfer coefficient G_{sl} plotted as a function of spin temperature T_s and lattice temperature T_l . In the limit of low T_s , the behavior of G_{sl} as a function of T_s is very close to being linear. At high T_s , G_{sl} increases and is maximum near the Curie temperature. At high T_s and high T_l , the data points become very scattered, but no significant new trend seem to emerge even at temperatures significantly higher than the Curie temperature.

all the spins are fully collinear. In this case any perturbation of the exchange coupling function J_{ij} still does not alter the directions of the effective exchange fields $\{\mathbf{H}_i\}$, which remain fully collinear with the spins, and hence do not induce any spin fluctuations.

By mapping g_{sl} onto the 3TM, we write

$$g_{sl} = G_{sl}(T_s - T_l). \quad (74)$$

Figure 8 shows a plot of the spin-lattice heat transfer coefficient G_{sl} as a function of T_s . In the limit of low T_s , the behavior of G_{sl} as a function of T_s is very close to being linear, in agreement with the analytical investigation outlined above. At high T_s , G_{sl} increases and is maximum near the Curie temperature. At high T_s and high T_l , the data points become very scattered, but no significant new trend seems to emerge even at temperatures significantly higher than the Curie temperature. By exploring the low T_s and low T_l regime, the temperature-dependent values of the damping parameter γ_{sl} can be evaluated using Eq. (10), where the subscript “ el ” is replaced by “ sl .” We find that the value predicted by simulations is $\gamma_{sl} \approx 1.5 \times 10^{-20} T_s$ eV s/ \AA^2 . This value is approximately twice the value found using analytical formula Eq. (73), and the linear variation of γ_{sl} as a function of T_s is the same as that predicted by analytical calculations. The approximations employed in the derivation of Eq. (73) show that it is difficult to give a more accurate and reliable analytical estimate for γ_{sl} . For example, giving an estimate for the six-dimensional integral (69) involves using the long wavelength magnon approximation, which not only breaks down entirely in the vicinity of the Curie temperature, but also does not approximate well the magnon dispersion relation in the vicinity of the Brillouin zone boundary. Still, the analytical result agrees well with direct numerical simulations and shows the same linear variation of $\gamma_{sl}(T)$ with temperature, namely $\gamma_{sl}(T) \sim T$.

VI. CONCLUSIONS

In this paper we have developed a dynamic spin-lattice-electron model for simulating the time-dependent evolution of coupled spin, atomic, and electronic degrees of freedom in a magnetic material. We first revisited the lattice-electron dynamic (LED) model, and derived it using the Furutsu-

Novikov theorem. Then, we developed a spin-lattice-electron dynamics (SLED) model, where the spin and lattice equations of motion are coupled to the heat transfer equation with diffusion term for the electronic subsystem. We have established how to relate the dissipative parameters entering the Langevin equations for the lattice and spin degrees of freedom to the heat transfer coefficients of a phenomenological spin-lattice-electron three-temperature model (3TM). We then applied the SLED model to the simulation of laser-induced demagnetization of iron thin films, and estimated the rates of heat transfer between the spins and electrons, and atoms and electrons. We proposed a way of separating the local collective motion of atoms from their random thermal motion, to enable us to model the dynamics of energy dissipation in a magnetic, or even nonmagnetic, material undergoing plastic deformation without introducing overdamping in the lattice subsystem. Using the SLED algorithm, we have simulated the propagation of compressive shock waves through magnetic iron, showing the possibility of incorporating the magnetic effects in dynamic simulations of mechanical deformation of a magnetic material. We have also explored the microscopic dynamics of dissipative coupling between the spin and lattice subsystems, and found that the rate of spin-lattice heat transfer is proportional to the integral of the four-spin time-dependent correlation function. At low temperatures, the spin-lattice energy transfer coefficient is a linear function of the spin temperature.

ACKNOWLEDGMENTS

This work was funded by Grant 534409 from the Hong Kong Research Grant Commission, and by the European Communities under the contract of Association between EURATOM and CCFE, where it was carried out within the framework of the European Fusion Development Agreement (EFDA). The views and opinions expressed herein do not necessarily reflect those of the European Commission. This work was also part-funded by the RCUK Energy Programme under Grant EP/I501045. P.-W.M. and S.L.D. acknowledge support from the EURATOM staff mobility programme, and support provided by the EPSRC via programme Grant EP/G050031.

*Leo.Ma@ccfe.ac.uk

- ¹F. Körmann, A. Dick, B. Grabowski, B. Hallstedt, T. Hickel, and J. Neugebauer, *Phys. Rev. B* **78**, 033102 (2008).
- ²F. Körmann, A. Dick, T. Hickel, and J. Neugebauer, *Phys. Rev. B* **81**, 134425 (2010).
- ³F. Körmann, A. Dick, T. Hickel, and J. Neugebauer, *Phys. Rev. B* **83**, 165114 (2011).
- ⁴V. P. Antropov, M. I. Katsnelson, B. N. Harmon, M. van Schilf-gaarde, and D. Kusnezov, *Phys. Rev. B* **54**, 1019 (1996).
- ⁵G. Kresse and J. Hafner, *Phys. Rev. B* **47**, 558 (1993).
- ⁶V. P. Antropov, M. I. Katsnelson, M. van Schilf-gaarde, and B. N. Harmon, *Phys. Rev. Lett.* **75**, 729 (1995).
- ⁷V. P. Antropov, *Phys. Rev. B* **72**, 140406 (2005).
- ⁸A. I. Lichtenstein, M. I. Katsnelson, and G. Kotliar, *Phys. Rev. Lett.* **87**, 067205 (2001).
- ⁹P.-W. Ma, C. H. Woo, and S. L. Dudarev, *Phys. Rev. B* **78**, 024434 (2008); also in *Electron Microscopy and Multiscale Modeling*, edited by A. S. Avilov *et al.*, AIP Conf. Proc. No. 999 (AIP, New York, 2008), p. 134.
- ¹⁰M. W. Finnis, P. Agnew, and A. J. E. Foreman, *Phys. Rev. B* **44**, 567 (1991).
- ¹¹A. Caro and M. Victoria, *Phys. Rev. A* **40**, 2287 (1989).
- ¹²D. M. Duffy and A. M. Rutherford, *J. Phys.: Condens. Matter* **19**, 016207 (2007); *J. Nucl. Mater.* **386**, 19 (2009).
- ¹³C. P. Race, D. R. Mason, M. W. Finnis, W. M. C. Foulkes, A. P. Horsfield, and A. P. Sutton, *Rep. Prog. Phys.* **73**, 116501 (2010).
- ¹⁴C. P. Race, D. R. Mason, and A. P. Sutton, *J. Phys.:Condens. Matter* **21**, 115702 (2009).
- ¹⁵S. Chandrasekhar, *Rev. Mod. Phys.* **15**, 1 (1943).
- ¹⁶R. Kubo, *Rep. Prog. Phys.* **29**, 255 (1966).
- ¹⁷W. Coffey, Yu. P. Kalmykov, J. T. Waldron, *The Langevin Equation*, 2nd ed. (World Scientific, Singapore, 2004).
- ¹⁸W. F. Brown Jr., *Phys. Rev.* **130**, 1677 (1963).
- ¹⁹J. L. García-Palacios and F. J. Lázaro, *Phys. Rev. B* **58**, 14937 (1998).
- ²⁰V. P. Antropov, S. V. Tretyakov, and B. N. Harmon, *J. Appl. Phys.* **81**, 3961 (1997).
- ²¹A. Lyberatos, D. V. Berkov, and R. W. Chantrell, *J. Phys.: Condens. Matter* **5**, 8911 (1993).
- ²²A. Lyberatos and R. W. Chantrell, *J. Appl. Phys.* **73**, 6501 (1993).
- ²³V. Tsiantos, W. Scholz, D. Suess, T. Schrefl, and J. Fidler, *J. Mag. Mag. Mater.* **242**, 999 (2002).
- ²⁴O. Chubykalo, R. Smirnov-Rueda, J. M. Gonzalez, M. A. Wongsam, R. W. Chantrell, and U. Nowak, *J. Mag. Mag. Mater.* **266**, 28 (2003).
- ²⁵V. Tsiantos, T. Schrefl, W. Scholz, H. Forster, D. Suess, R. Dittrich, and J. Fidler, *IEEE Trans. Mag.* **39**, 2507 (2003).
- ²⁶P.-W. Ma and S. L. Dudarev, *Phys. Rev. B* **83**, 134418 (2011).
- ²⁷P.-W. Ma, S. L. Dudarev, A. A. Semenov, and C. H. Woo, *Phys. Rev. E* **82**, 031111 (2010).
- ²⁸B. Skubic, J. Hellsvik, L. Nordström, and O. Eriksson, *J. Phys.: Condens. Matter* **20**, 315203 (2008).
- ²⁹I. Radu, K. Vahaplar, C. Stamm, T. Kachel, N. Pontius, H. A. Dürr, T. A. Ostler, J. Barker, R. F. L. Evans, R. W. Chantrell, A. Tsukamoto, A. Itoh, A. Kirilyuk, Th. Rasing, and A. V. Kimel, *Nature (London)* **472**, 205 (2011).
- ³⁰E. Beaurepaire, J.-C. Merle, A. Daunois, and J.-Y. Bigot, *Phys. Rev. Lett.* **76**, 4250 (1996).
- ³¹B. Koopmans, G. Malinowski, F. Dalla Longa, D. Steiauf, M. Fähnle, T. Roth, M. Cinchetti, and M. Aeschlimann, *Nat. Mater.* **9**, 259 (2010).
- ³²E. Carpene, E. Mancini, C. Dallera, M. Brenna, E. Puppini, and S. De Silvestri, *Phys. Rev. B* **78**, 174422 (2008).
- ³³B. Koopmans, J. J. M. Ruigrok, F. Dalla Longa, and W. J. M. de Jonge, *Phys. Rev. Lett.* **95**, 267207 (2005).
- ³⁴C. Stamm, T. Kachel, N. Pontius, R. Mitzner, T. Quast, K. Holldack, S. Khan, C. Lupulescu, E. F. Aziz, M. Wietstruk, H. A. Dürr, and W. Eberhardt, *Nat. Mater.* **6**, 740 (2007).
- ³⁵C. Stamm, N. Pontius, T. Kachel, M. Wietstruk, and H. A. Dürr, *Phys. Rev. B* **81**, 104425 (2010).
- ³⁶J.-Y. Bigot, M. Vomir, and E. Beaurepaire, *Nat. Phys.* **5**, 515 (2009).
- ³⁷G. P. Zhang, W. Hübner, G. Kefkidis, Y. Bai, and T. F. George, *Nat. Phys.* **5**, 499 (2009).
- ³⁸G. P. Zhang, *J. Phys.: Condens. Matter* **23**, 206005 (2011).
- ³⁹W. Hübner and G. P. Zhang, *Phys. Rev. B* **58**, R5920 (1998).
- ⁴⁰M. Fähnle, J. Seib, and C. Illg, *Phys. Rev. B* **82**, 144405 (2010).
- ⁴¹P.-W. Ma and C. H. Woo, *Phys. Rev. E* **79**, 046703 (2009).
- ⁴²K. Kadau, T. C. Germann, P. S. Lomdahl, and B. L. Holian, *Science* **296**, 1681 (2002); *Phys. Rev. B* **72**, 064120 (2005).
- ⁴³A. F. Calder, D. J. Bacon, A. V. Barashev and Yu. N. Osetsky, *Philos. Mag.* **90**, 863 (2010); *Philos. Mag. Lett.* **88**, 43 (2008).
- ⁴⁴H. Hasegawa and D. G. Pettifor, *Phys. Rev. Lett.* **50**, 130 (1983).
- ⁴⁵M. Y. Lavrentiev, D. Nguyen-Manh, and S. L. Dudarev, *Phys. Rev. B* **81**, 184202 (2010).
- ⁴⁶D. Nguyen-Manh, A. P. Horsfield, and S. L. Dudarev, *Phys. Rev. B* **73**, 020101 (2006).
- ⁴⁷P. M. Derlet, D. Nguyen-Manh, and S. L. Dudarev, *Phys. Rev. B* **76**, 054107 (2007).
- ⁴⁸S. L. Dudarev, R. Bullough, and P. M. Derlet, *Phys. Rev. Lett.* **100**, 135503 (2008).
- ⁴⁹Z. Yao, M. L. Jenkins, M. Hernandez-Mayoral, and M. A. Kirk, *Philos. Mag.* **90**, 4623 (2010).
- ⁵⁰S. P. Fitzgerald and S. L. Dudarev, *Proc. R. Soc. A* **464**, 2549 (2008).
- ⁵¹P.-W. Ma, C. H. Woo, and S. L. Dudarev, *Philos. Mag.* **89**, 2921 (2009).
- ⁵²C. H. Woo, in *Handbook of Materials Modelling*, edited by S. Yip (Springer, Berlin, 2005), pp. 959–986.
- ⁵³K. Furutsu, *J. Res. Natl. Bur. Stand. D* **67**, 303 (1963).
- ⁵⁴E. A. Novikov, *Zh. Eksp. Theor. Fiz* **47**, 1919 (1964) [*Sov. Phys. JETP* **20**, 1290 (1965)].
- ⁵⁵I. Cook, *Plasma Phys.* **20**, 349 (1978).
- ⁵⁶A. Ishimaru, *Wave Propagation and Scattering in Random Media* (Academic, New York, 1978).
- ⁵⁷The Furutsu-Novikov Theorem^{53–56} states that the ensemble average of a product of a functional $f(t)$, depending on Gaussian noise $\epsilon(t)$, and the noise itself, equals $\langle \epsilon(t)f(t) \rangle = \int dt' \langle \epsilon(t)\epsilon(t') \rangle \langle \delta f(t) / \delta \epsilon(t') \rangle$, where $\delta f(t) / \delta \epsilon(t')$ denotes a functional derivative.
- ⁵⁸E. M. Lifshitz and L. P. Pitaevskii, *Physical Kinetics* (Pergamon, Oxford, United Kingdom, 1981), pp. 17–21.
- ⁵⁹D. Forster, *Hydrodynamic Fluctuations, Broken Symmetry, and Correlation Functions* (W. A. Benjamin, London, 1975).
- ⁶⁰M. van Schilf-gaarde and V. A. Antropov, *J. Appl. Phys.* **85**, 4827 (1999).
- ⁶¹I. Turek, J. Kudrnovsky, V. Drchal, and P. Bruno, *Philos. Mag.* **86**, 1713 (2006).

- ⁶²S. V. Okatov, Yu. N. Gornostyrev, A. I. Lichtenstein, and M. I. Katsnelson, *Phys. Rev. B* **84**, 214422 (2011).
- ⁶³W. Marshall and S. W. Lovesey, *Theory of Thermal Neutron Scattering* (Clarendon, Oxford, 1971).
- ⁶⁴S. W. Lovesey, *Theory of Neutron Scattering from Condensed Matter* (Clarendon, Oxford, 1984), Vols. 1 and 2.
- ⁶⁵S. L. Dudarev and P. M. Derlet, *J. Phys.: Condens. Matter* **17**, 1 (2005).
- ⁶⁶C. Björkas and K. Nordlund, *Nucl. Instrum. Methods Phys. Res. Sect. B* **259**, 853 (2007).
- ⁶⁷L. D. Landau and E. M. Lifshitz, *Fluid Mechanics* (Butterworth-Heinemann, Oxford, 2000).
- ⁶⁸W. Kohn, *Phys. Rev. Lett.* **76**, 3168 (1996).
- ⁶⁹E. Prodan and W. Kohn, *Proc. Natl. Acad. Sci. USA* **102**, 11635 (2005).
- ⁷⁰R. Zwanzig, *Nonequilibrium Statistical Mechanics* (Oxford University Press, New York, 2001).
- ⁷¹N. G. Van Kampen, *Stochastic Processes in Physics and Chemistry* (North-Holland, Amsterdam, 1981).
- ⁷²N. Hatano and M. Suzuki, *Lect. Notes Phys.* **679**, 37 (2005).
- ⁷³I. P. Omelyan, I. M. Mryglod, and R. Folk, *Phys. Rev. Lett.* **86**, 898 (2001).
- ⁷⁴I. P. Omelyan, I. M. Mryglod, and R. Folk, *Phys. Rev. E* **66**, 026701 (2002).
- ⁷⁵S.-H. Tsai, H. K. Lee, and D. P. Landau, *Brazilian J. Phys.* **34**, 384 (2004).
- ⁷⁶S.-H. Tsai, H. K. Lee and D. P. Landau, *Am. J. Phys.* **73**, 615 (2005).
- ⁷⁷B. L. Holian, W. G. Hoover, B. Moran, and G. K. Straub, *Phys. Rev. A* **22**, 2798 (1980).
- ⁷⁸B. L. Holian and P. S. Lomdahl, *Science* **280**, 2085 (1998).
- ⁷⁹C. Kittel, *Introduction to Solid State Physics*, 7th ed. (Wiley, New York, 1996), p. 157.
- ⁸⁰S. L. Dudarev, *Phys. Rev. B* **65**, 224105 (2002); *C. R. Phys.* **9**, 409 (2008).
- ⁸¹J. P. Perdew, K. Burke, and M. Ernzerhof, *Phys. Rev. Lett.* **77**, 3865 (1996).
- ⁸²S. Chiesa, P. M. Derlet, and S. L. Dudarev, *Phys. Rev. B* **79**, 214109 (2009).